cosmetics

MDPI

Article

The Effects of Bio-Based Succinic Acid vs. Salicylic Acid on Stratum Corneum Desquamation and Human Skin Barrier Function

Géraldine Louvet-Pommier [1,*,†], Yuanyuan Fang [2,†], Qian Zhang [2], Mengxue Gao [2], Xiaowei Chang [2,*], Daniel Wils [3] and Damien Truffin [3]

[1] Cosmetic Expertise Center of Roquette, 93210 Saint-Denis, France
[2] Shanghai R&D Center of Proya Cosmetics Co., Ltd., Shanghai 200233, China; fangyuanyuan13@proya.com (Y.F.); zhangqian63@proya.com (Q.Z.); gaomengxue@proya.com (M.G.)
[3] Roquette Frères, Nutrition and Health Research, 62136 Lestrem, France; damien.truffin@roquette.com (D.T.)
* Correspondence: geraldine.louvet-pommier@roquette.com (G.L.-P.); changxiaowei@proya.com (X.C.)
† These authors contributed equally to this work.

Abstract

Bio-based succinic acid (bSU) has emerged as a promising mild exfoliating agent, yet its effects on desquamation pathways, barrier-related protein regulation, and irritation potential remain insufficiently characterized in human-relevant skin models. Therefore, this study systematically evaluated bSU against salicylic acid (SA) using reconstructed human epidermis and human skin explants to assess irritation profile and desquamation-related biological responses. Our findings reveal that bSU facilitates controlled corneocyte shedding by modulating the targets LEKTI, KLK, and CDSN. Moreover, bSU demonstrated a favorable ability to maintain physiological skin surface acidity, all while minimizing inflammatory activation. These results position bSU as a balanced exfoliating bioactive that effectively promotes stratum corneum renewal while preserving cutaneous barrier homeostasis, providing mechanistic insights to support its development in advanced mild exfoliation formulations.

Keywords: succinic acid; desquamation; corneodesmosomes; epidermal barrier; mild exfoliation

1. Introduction

The stratum corneum (SC), the outermost epidermis layer, provides an essential barrier against chemical, biological, and physical assaults [1]. The SC undergoes continuous renewal through tightly coordinated processes of keratinocyte proliferation, differentiation, and desquamation to maintain skin homeostasis and integrity, as its dysregulation may lead to various dermatological conditions [2–4].

The precise regulation of SC desquamation primarily revolves around the LEKTI-KLK protease axis [5,6]. Kallikrein-related peptidases (KLKs), particularly KLK5, KLK7, and KLK14, are secreted by granular keratinocytes and promote corneocyte desquamation by selectively degrading corneodesmosomal adhesive proteins [7,8]. Their activity is counterbalanced by the protease inhibitor Lympho-Epithelial Kazal-Type-related Inhibitor (LEKTI), which prevents excessive desquamation through precise regulation of protease activation [9,10]. Within this proteolytic cascade, the glycoprotein corneodesmosin (CDSN) serves as a critical structural component of corneodesmosomes. Its deficiency leads to aberrant desquamation and barrier impairment [11–13]. Meanwhile, Desmoglein 1 (DSG1) in the viable epidermis maintains epidermal integrity through desmosomal stabilization,

Check for updates

Academic Editor: Enzo Berardesca

Received: 26 January 2026
Revised: 25 March 2026
Accepted: 30 April 2026
Published: 13 May 2026

Copyright: © 2026 by the authors. Licensee MDPI, Basel, Switzerland. This article is an open access article distributed under the terms and conditions of the Creative Commons Attribution (CC BY) license.

and its controlled degradation ensures orderly corneocyte shedding [14,15]. The balance of this sophisticated regulatory system is decisive for maintaining normal skin barrier function and homeostasis. Its dysregulation leads to various pathological states, as exemplified by Netherton syndrome, where LEKTI deficiency results in uncontrolled KLK protease activity, premature DSG1 degradation, and severe barrier impairment [16].

Moderate chemical exfoliation can effectively address skin concerns caused by corneocyte accumulation, such as roughness, dullness, and impaired product absorption [17,18]. Studies demonstrate that 30% supramolecular salicylic acid (SA) improves skin barrier function while effectively exfoliating with acne treated [19]. Current chemical exfoliants are primarily categorized into alpha-hydroxy acids (e.g., glycolic acid, lactic acid), beta-hydroxy acids (represented by SA), and polyhydroxy acids (e.g., gluconolactone) [20,21]. SA exhibits amphiphilic properties due to the presence of both an aromatic ring and polar functional groups, enabling effective pore penetration and removal of excess sebum and corneocytes [22]. However, growing evidence indicates that SA can cause skin irritation and barrier damage [23], leading to strict concentration limits in cosmetic products. These constraints drive the industry to seek safer, gentler alternatives. AHAs are effective in promoting superficial peeling and improving keratosis and acne. However, their biological effects appear to be highly concentration-dependent. High concentrations can disrupt corneocyte cohesion, compromise barrier integrity, and induce adverse reactions, such as burning, swelling, and pruritus. Although the clinical efficacy of acid-based exfoliants has been documented, mechanistic investigations at the molecular level remain relatively limited. Most available evidence focuses on clinical outcomes or histological observations, whereas detailed elucidation of desquamation-related pathways, such as KLK-mediated proteolysis or differentiation-associated signaling networks, is comparatively scarce [24].

Succinic acid is a naturally occurring organic acid that has been reported to possess properties beneficial to skin health, including regulating sebum secretion, antioxidant, anti-inflammatory, and antimicrobial effects [25–28]. Studies have demonstrated that the combination of succinic acid with hyaluronic acid can enhance the regenerative capacity of senescent adipocytes at the cellular level [29]. Bio-based succinic acid (bSU) produced through bioprocessing, possesses a unique four-carbon short-chain structure and dual carboxylic acid groups, conferring mild properties while maintaining efficacy. It also exhibits inherent antimicrobial activity, making it a promising novel bioactive substance [30]. Preliminary investigations have revealed that bSU, like α-hydroxy acids, has the ability to modulate keratinocyte metabolism. However, systematic comparative studies on bSU regarding its exfoliation efficacy and skin compatibility remain scarce, particularly concerning its impact on key desquamation-related proteins.

This study aims to systematically evaluate the practical application value of bSU as an exfoliating ingredient. Utilizing both a SkinEthic™ reconstructed human epidermis (RHE) model and ex vivo skin explants [31–33], bSU and SA were comprehensively compared across multiple dimensions, including epidermal morphological changes, expression of key desquamation markers, and skin barrier function, providing scientific evidence for bSU as a mild and effective exfoliating component.

2. Materials and Methods

2.1. Materials

2.1.1. Test Materials

SA was obtained from Laboratoire Cooper, France (batches 15090067/C and 18060139/1). bSU (Beauté by Roquette® SA 130, batches S0778 and S1204) was provided by Roquette Frères, France. For all experiments, SA and bSU were prepared in sterile demineralized water to final concentrations of 0.8%, 1%, and 3% (*w*/*w*). Concentrations

of 0.8% and 1.0% were selected as representative low concentrations to assess mildness as the first objective, along with peeling efficacy, while 3% concentration was chosen to maximize the peeling effect and irritation to assess the difference between bSU and SA. The SA solution was freshly prepared prior to each sample application and solubilized using ultrasonic assistance, with no unstable phenomena, such as precipitation, observed during sample application. A study was also performed to evaluate the stability of SA and bSU aqueous solutions (1 and 2%) after 3 months of daylight exposure: bSU showed no yellowing of the formula after 3 months of exposure to daylight compared to SA. Solution of SA 2% was slightly more yellow. No separation was observed for all solutions of bSU and SA.

Sterile demineralized water served as the vehicle control, while 2% sodium dodecyl sulfate (SDS, positive control) was used where specified.

2.1.2. Biological Models

The RHE model (SkinEthic™ RHE/S/17, EPISKIN, Lyon, France) was used for all in vitro assays. Tissues were maintained in 6-well plates containing 1 mL of SkinEthic™ maintenance medium (EPISKIN, France) and incubated at 37 °C, 5% CO_2, and 95% relative humidity (MCO-18AIC, PHCbi). Human skin explants were obtained from abdominoplasty surgical residues following written informed consent from donors, in accordance with the Declaration of Helsinki and Article L.1243-4 of the French Public Health Code. The latter does not require any prior authorization from an ethics committee for sampling and using surgical waste. Explants (diameter 12 and 38 mm) were derived from two Caucasian female donors aged 66 and 43 years, respectively. Samples were maintained ex vivo in BIO-EC's Explants Medium (BEM) at 37 °C in a humidified atmosphere with 5% CO_2.

2.2. In Vitro Studies on RHE

2.2.1. Cell Viability

The RHE tissues (n = 3 per group) were topically treated with 20 µL of the test solutions or the vehicle control for 20 h of incubation at 37 °C. Sodium dodecyl sulfate (SDS) at 2% in water served as the positive control for cytotoxicity. Cell viability was assessed via the MTT (3-(4,5-dimethylthiazol-2-yl)-2,5-diphenyltetrazolium bromide) assay. The reduction of MTT to insoluble purple formazan by mitochondrial succinate dehydrogenase was quantified. The formed formazan crystals were solubilized, and absorbance was measured at 570 nm using a VMAX microplate reader (Molecular Devices, San Jose, CA, USA). Viability was expressed as a percentage relative to the untreated control (set as 100%).

2.2.2. Inflammation Marker Assay

RHE tissues were treated with 25 µL of test substances for 24 h. Subsequently, 2 mL of the epidermal tissue culture fluid was collected in a centrifuge tube, centrifuged at 12,000 RPM for 5 min (Eppendorf® 5804R, Hamburg, Germany), and stored at −80 °C. Cytokine levels (Interleukin 1 alpha (IL-1α), Interleukin 8 (IL-8), and Prostaglandin E2 (PGE2)) were quantified using commercial ELISA kits (Abcam, Cambridge, UK; Ray-Biotech, Peachtree Corners, GA, USA) in accordance with the instructions provided by the manufacturers. Absorbance was measured at 450 nm [34].

2.2.3. In Vitro Exfoliation Assay

To evaluate the exfoliation potential, the RHE surface was gently rubbed with a syringe rubber sieve (using the rubber stopper of the syringe to simulate the rubbing action during daily hand contact with human skin, which corresponds to the mechanical exfoliation of the stratum corneum during face washing—the entire experiment was performed by one lab operator to ensure consistency) for 2 min to dislodge loosened corneocytes. using

the rubber stopper of a syringe to simulate the rubbing action during daily hand contact with human skin, which corresponds to the mechanical exfoliation of the stratum corneum during face washing. The entire experiment was performed by one lab operator to ensure consistency. The surface was then rinsed with 500 µL of 0.1% Triton X-100, and the eluate was collected. The protein concentration in the eluate, reflecting the number of exfoliated corneocytes, was quantified using the Pierce™ BCA Protein Assay Kit (Thermo Fisher Scientific, Waltham, MA, USA).

2.2.4. Histological and Immunofluorescence Analysis

RHE tissues were fixed with 4% neutral buffered formaldehyde (Beyotime Biotech, Shanghai, China) at 4 °C overnight, then dehydrated with a graded ethanol and embedded in paraffin using an embedding machine (JB-P5, Wuhan Junjie Electronics Co., Ltd., Wuhan, China). Subsequently, 5-µm-thick tissue sections were cut by a Pathology slicer (Leica RM2016) and mounted on glass slides. Hematoxylin and eosin (H&E) staining was performed to assess tissue morphology, and images were acquired using an inverted fluorescence microscope (Nikon Ts2R-FL, Tokyo, Japan). For immunofluorescence, paraffin sections were dewaxed, rehydrated, and subjected to antigen retrieval. Sections were incubated with primary antibodies targeting CDSN, DSG1, KLK7, Keratin 1 (K1), Keratin 10 (K10) (Abcam, UK), and LEKTI (Thermo Fisher Scientific, USA), followed by appropriate fluorescent secondary antibodies. Nuclei were counterstained with DAPI (Abcam). Images were captured under a fluorescence microscope, and the fluorescence area was quantified using Image Software (version 1.52e). For each condition, at least three independent specimens were analyzed under identical exposure parameters [34].

2.3. Ex Vivo Studies on Human Skin Explants

2.3.1. Explants Treatment

Explants were cultured on biocompatible grids at the air-liquid interface in BEM at 37 °C, 5% CO_2. The culture medium (1 mL) was partially renewed every 48 h. The experimental design included a baseline Tissue Control group harvested at day 0 (D0), an Untreated Control group cultured without intervention, and treatment groups (n = 3 per group). Treatments (SA, bSU, or vehicle) were applied topically at a dose of 2 µL/explant (≈2 mg/cm^2) on D0, D3, and D5.

2.3.2. Skin Surface pH and Transepidermal Water Loss (TEWL) Measurements

Skin surface pH was measured using a PH-METER 905® (Courage & Khazaka electronics, Cologne, Germany). Measurements were taken at the following time points: baseline (D0) before the first treatment; 6 h after each treatment on D0, D3, and D5 (after wiping the explants), and 24 h after each treatment on D1, D4, and D6. The TEWL measurements were performed during the survival of skin explants at different time points: D0, D1, D4, D5, and D6, before treatment using VapoMeter® SWL5 (Delfin Technologies, Kuopio, Finland), with three replicates per explant.

2.3.3. Sample Harvesting and Histological Processing

On the last day of the experiment (D6), all explants, including T0 controls, were harvested. Each explant was bisected. One half was fixed in buffered formalin for subsequent histological and immunohistochemical analysis, while the other half was snap-frozen in liquid nitrogen and stored at −80 °C for subsequent analyses. Formalin-fixed specimens were dehydrated through a graded ethanol series, cleared in xylene, and embedded in paraffin using an automated tissue processor (Leica PEARL, Leica biosystems, Nanterre, France). Sections (5 µm) were cut using a rotary microtome (Leica RM2125, Leica biosystems, France) and mounted on glass slides. Frozen specimens were sectioned at 7 µm using

a cryostat (Leica CM3050S, Leica biosystems, France). All sections were evaluated under light microscopy (Leica DMLB or Olympus BX43).

2.3.4. Histomorphological Analysis

Cell viability of epidermal and dermal structures was observed on paraffin sections stained with Masson's trichrome Goldner variant. SC thickness (µm) was measured on digital images captured from Masson's trichrome-stained sections, using the measurement module of Olympus CellD software (version 3.4; Olympus, Tokyo, Japan). The number of corneocyte layers was determined on frozen sections processed using the Mackenzie technique. Briefly, sections were treated with sodium hydroxide solution to induce corneocyte swelling. Images were acquired, and the number of distinct corneocyte layers was counted on each image using Olympus CellD software.

2.3.5. Immunostaining Assay

Both immunohistochemistry (IHC) and immunofluorescence (IF) were performed on 5 µm-FFPE (formalin-fixed, paraffin-embedded) skin sections or 7 µm-frozen sections. Polyclonal anti-CDSN antibody (Sigma, Ref. HPA044730, SIGMA, Lezennes, France) and anti-LEKTI antibody (Novus Biologicals, Ref. NBP1-90510, NOVUS, Bernouville, France) were used for IHC staining, amplified with a biotin-streptavidin system, and revealed with a violet peroxidase substrate (Vector, Ref. SK-4600, Santa Cruz Biotechnologies, Heidelberg, Germany). Polyclonal anti-DSG1 antibody (SantaCruz, Ref. sc-20114, Santa Cruz Biotechnologies, Germany) was used for IF staining, amplified with a biotin-streptavidin-AF488 system (Life Technologies, Ref. SK-A11008, Life Technologies, Fischer Scientific, Courtaboeuf, France). All immunostaining procedures were carried out using an automated system (Autostainer, Dako, Les Ulis, France), and the resulting labelling was assessed by qualitative and semi-quantitative microscopic examination.

2.4. Statistical Analysis

All the data were expressed as mean ± SD and analyzed using one-way ANOVA with Tukey's post hoc test or two-way ANOVA with Dunnett's post hoc test. A value of $p < 0.05$ was considered as statistically significant; non-significant results were denoted as "ns."

3. Results and Discussions

3.1. Evaluation of the Exfoliating Effects of bSU in the RHE Model

3.1.1. Exfoliation Efficacy and Morphology

H&E staining was performed on tissue cross-sections to evaluate the structural alterations in the treated SC. Prior to application, the working solutions of bSU and SA were adjusted to comparable pH values (3.6 ± 0.2) to ensure controlled experimental conditions. Compared with the control group, treatment with 1% bSU or 1% SA increased SC thickness and enhanced lamellar organization (Figure 1a). The bSU-treated specimens exhibited a significant increase in SC thickness (Figure 1b). Notably, widened intercellular spaces and looser inter-lamellar structure were observed within the SC, while maintaining complete epidermal integrity. In contrast, mild vacuolization and disorganization of keratinocytes were evident in the SA-treated group, suggesting subtle damage to viable keratinocytes. Both groups showed a significant reduction in viable epidermal cell-layer thickness, with no significant difference between the groups (Figure 1c).

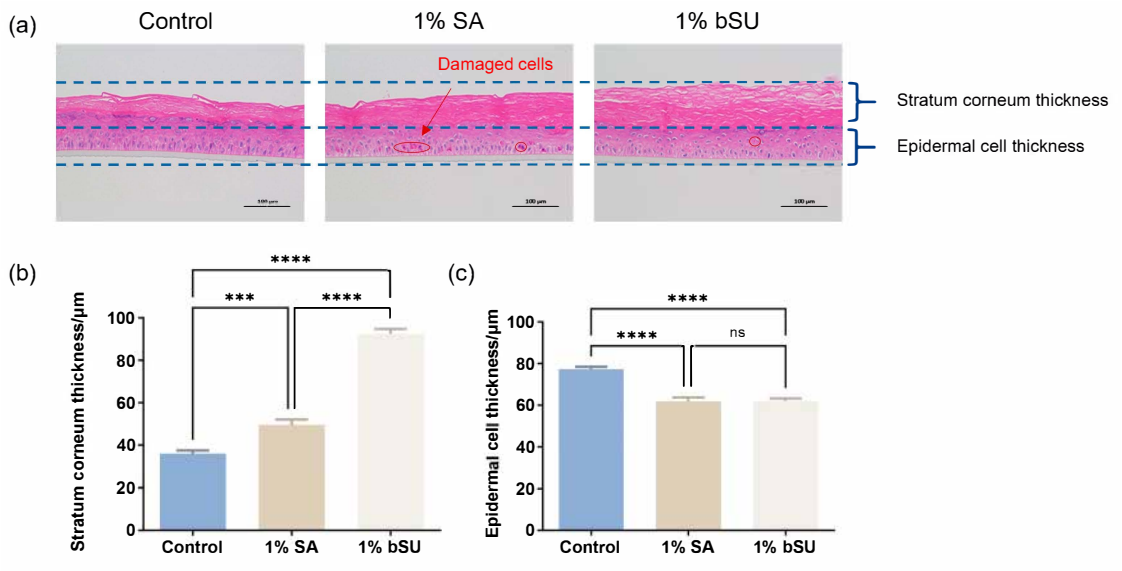

Figure 1. Comparison of the RHE model after treatment with 1% SA or 1% bSU vs. the Control. (**a**) H&E staining; (**b**) SC thickness; (**c**) viable epidermal cell layer thickness. $n = 3$. *** $p < 0.001$; **** $p < 0.0001$, ns: non-significant.

To quantitatively assess the exfoliation efficacy of SA and bSU, the shed keratinocytes were collected, and the total protein content in eluates from treated skin models was quantified using the BCA assay. The amount of exfoliated cells as a reliable indicator of keratinocyte desquamation can be characterized which represents the exfoliation capacity [10]. Results showed that treatment with 1% SA and 1% bSU significantly increased the protein concentration in the eluate compared with the control, indicating enhanced keratinocyte shedding. Notably, no statistically significant difference was observed between the two treatments at the same concentration, suggesting comparable exfoliation efficacy (Figure 2).

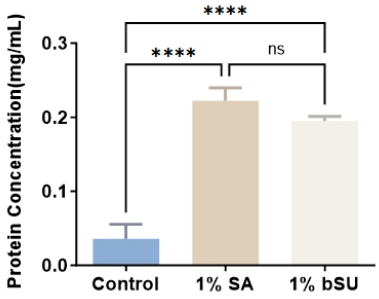

Figure 2. Protein concentration in exfoliated keratinocytes (BCA protein assay) after treatment with 1% SA or 1% bSU vs. the Control. $n = 3$. **** $p < 0.0001$, ns: non-significant.

3.1.2. Cellular Differentiation, Homeostasis, and Inflammatory Response

The integrity of keratinocyte differentiation was evaluated through quantification of K1 and K10, which are structural proteins that form a network in the upper epidermal layers as key markers of epidermal differentiation [35]. Aberrant expression or localization of these proteins is associated with disruption of epidermal architecture [34,36]. Immunofluorescence analysis confirmed that neither bSU nor SA interfered with the expression of K1 or K10 compared to the control, indicating no disruption to the keratinocyte life cycle or differentiation process (Figure 3).

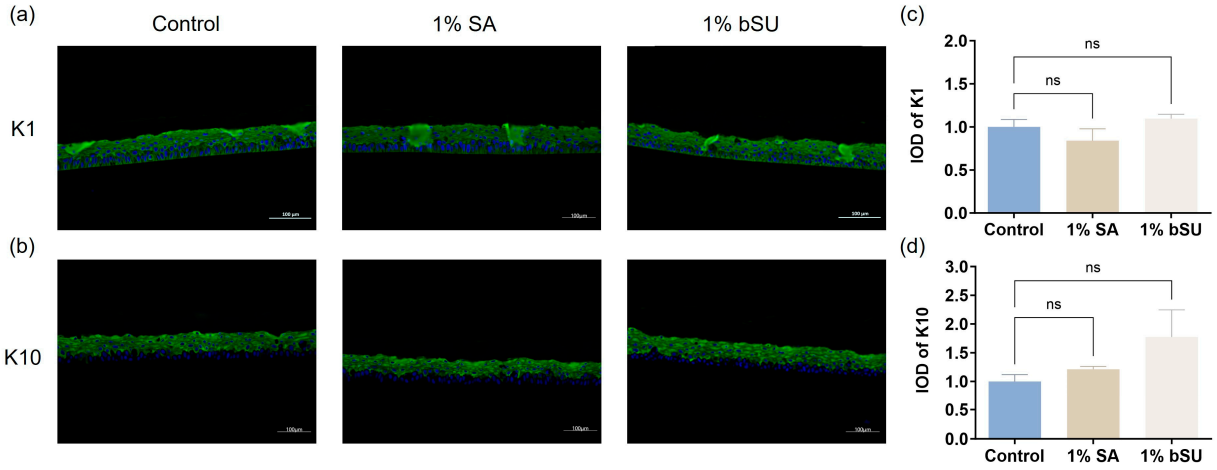

Figure 3. Immunofluorescence images of (**a**) K1 and (**b**) K10 in Control, 1% SA, and 1% bSU groups. Keratin staining is shown in green, and nuclei are counterstained with DAPI (blue); Integrated Optical Density (IOD) quantification of (**c**) K1 and (**d**) K10 expression. $n = 3$. ns: non-significant.

Further analysis of inflammatory biomarkers revealed distinct irritation profiles between the two compounds. At 1% concentration, both treatments increased IL-8 levels, with SA showing a greater increase than bSU. The bSU induced only minimal, non-significant increases in IL-1α, whereas SA statistically elevated IL-1α levels. No significant differences in PGE2 levels were detected across treatments (Figure 4).

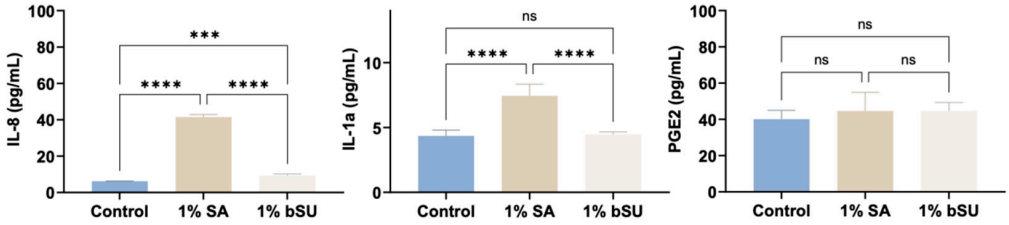

Figure 4. Effect of formulations on the expression of IL-8, IL-1α, and PGE2 after treatment with 1% SA or 1% bSU vs. Control. $n = 3$. *** $p < 0.001$; **** $p < 0.0001$.

3.1.3. Exfoliation Mechanism: Corneocyte Adhesion Proteins and Protease Cascade

Corneodesmosomal degradation, mediated by KLK5 and KLK7 in a pH-dependent manner [37,38], represents a central event in desquamation, involving regulated proteolysis of adhesion proteins including CDSN and DSG1 [12,13]. To investigate the regulatory effects of bSU and SA on keratinocyte adhesion and desquamation, immunofluorescence staining was performed to analyze the expression of adhesion- and protease system–related markers in the RHE model. Quantitative analysis revealed that both acids reduced CDSN expression, with a more pronounced decrease observed in the 1% bSU group (Figure 5a). Regarding DSG1, no significant difference was found between all groups. However, a directional decrease was observed with bSU, and its effect differed from that of SA (Figure 5b).

Analysis of protease-related biomarkers LEKTI and KLK7 revealed that, at a concentration of 1%, both bSU and SA treatments induced an upregulation of LEKTI protein expression (Figure 6a), accompanied by a decrease in KLK7 expression (Figure 6b). This outcome is inconsistent with the theoretical expectation that an acidic environment promotes the dissociation of the LEKTI–KLK complex and enhances KLK activity [10]. Such a discrepancy may be attributed to the physiological limitations of the RHE model in reproducing the native epidermal microenvironment.

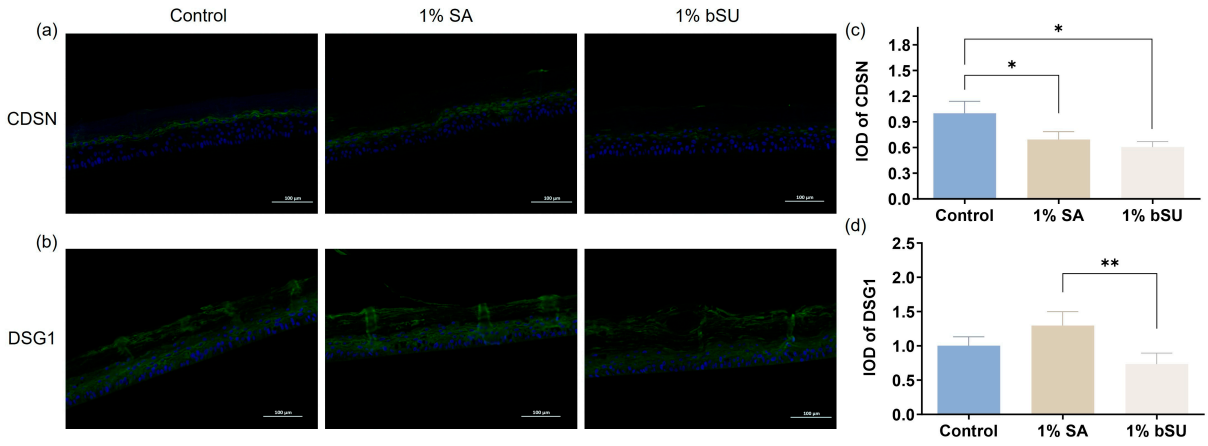

Figure 5. Immunofluorescence images of (**a**) CDSN and (**b**) DSG1 in Control, 1% SA, and 1% bSU groups. Keratin staining is shown in green, and nuclei are counterstained with DAPI (blue); IOD quantification of (**c**) CDSN and (**d**) DSG1 expression. * $p < 0.05$; ** $p < 0.01$.

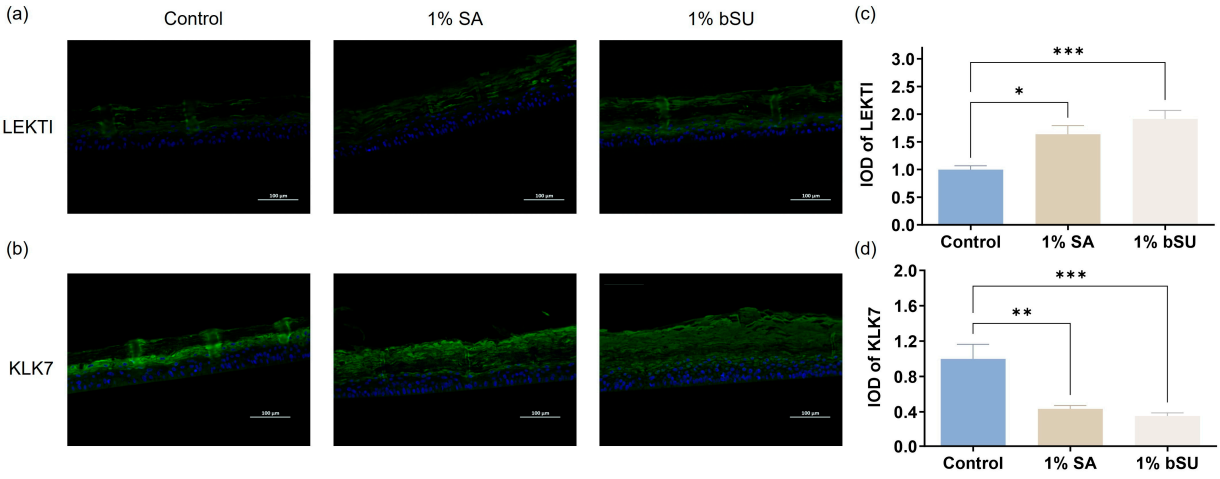

Figure 6. Immunofluorescence images of (**a**) LEKTI and (**b**) KLK7 in Control, 1% SA, and 1% bSU groups. Keratin staining is shown in green, and nuclei are counterstained with DAPI (blue); IOD quantification of (**c**) LEKTI and (**d**) KLK7 expression. * $p < 0.05$; ** $p < 0.01$; *** $p < 0.001$.

3.1.4. Impact on Filaggrin (FLG) Expression

FLG, a key protein effector, aggregates keratin filaments and is subsequently proteolytically processed into natural moisturizing factors, which are indispensable for SC hydration and acidity [39–41]. The impact of exfoliants on FLG expression was evaluated in the RHE model. Immunofluorescence analysis revealed that both acid treatments reduced FLG expression at an equivalent concentration. Notably, bSU performed better in maintaining FLG expression, although the difference did not reach statistical significance (Figure 7).

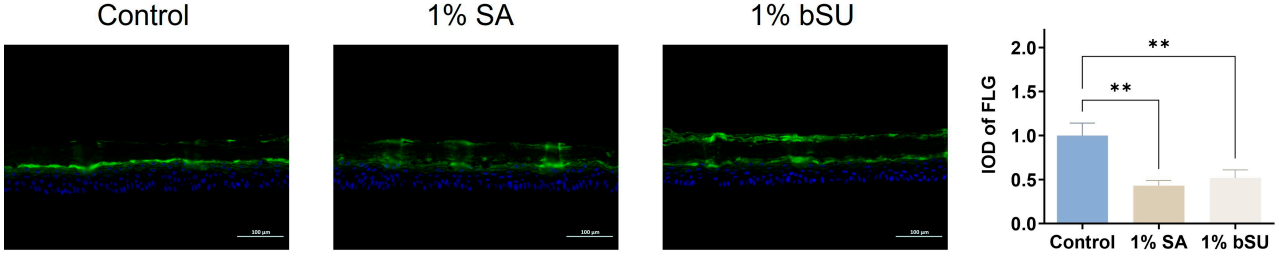

Figure 7. Immunofluorescence and IOD quantification of FLG expression in RHE after treatment with 1% SA and 1% bSU. $n = 3$. ** $p < 0.01$. Keratin staining is shown in green, and nuclei are counterstained with DAPI (blue).

3.2. Modulation of Tissue Homeostasis and Barrier Function by bSU in Human Skin Explants

To further validate and extend the RHE findings, an ex vivo human skin explant model was employed. This model preserves the native epidermal–dermal architecture and microenvironment [42], enabling a more physiologically relevant assessment of epidermal adhesion, desquamation, and barrier function. In addition, a 3% treatment was included to evaluate the dose-dependent effects of bSU and its capacity to maintain epidermal homeostasis without inducing cytotoxicity.

3.2.1. Histological Morphology and Cell Viability Assessment

Histological evaluation revealed that after six days of treatment, both 1% and 3% bSU maintained intact epidermal and dermal structures with no detectable tissue damage (Figure 8). The bSU induced a modest reduction in SC thickness (−21% at 1% and −10% at 3%) and a minor reduction in the scaly surface appearance, suggesting mild promotion of SC renewal while preserving tissue integrity. In contrast, SA increased SC thickness (+9% at 1% and +30% at 3%) and enhanced scaly, rough surface features (Table 1).

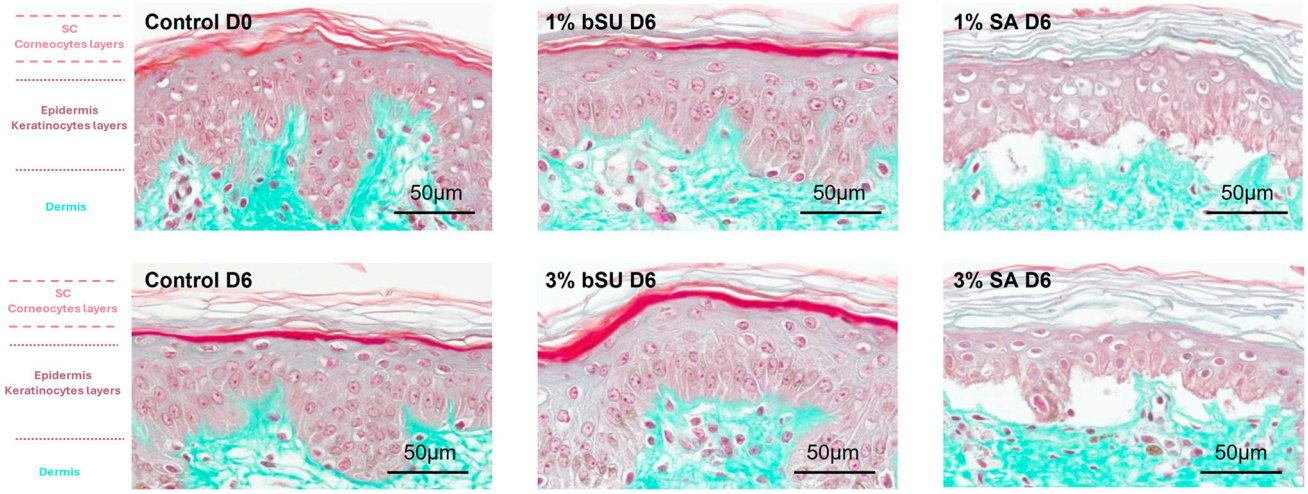

Figure 8. Effect of product application on skin explant morphology and cell viability, compared to control, on D6. $n = 3$.

Table 1. Summary of skin morphology variation after various treatments on skin explant of SA or bSU, vs. Control on D6. Observation from histological evaluation; $n = 3$. Depending on the intensity, the variations are expressed as follows: Light decrease: ↘; Light increase: ↗; Moderate decrease: ↘↘; Very clear decrease: ↘↘↘↘↘; No variation: ↔.

Skin Morphology Variations After Treatments vs Untreated Control on Day 6-Histological Observations.	SA 1%	bSU 1%	SA 3%	bSU 3%	SA 10%	bSU 10%
Cell viability/Tissue Viability	↘↘↘↘↘	↔	↘↘↘↘↘	↔	↘↘↘↘↘	↔
Stratum corneum thickness variation	9% #	−21% **	30% **	−10% **	Not measured	Not measured
Number of corneocytes layers variation	−12% NS	−4% NS	−3% NS	−4% NS	Not measured	Not measured
Stratum corneum morphology	↗Thickness ↗Flaky appearance	↘Thickness ↘↘Flaky appearance	↗Thickness ↗Flaky appearance Detachment by area	↘Thickness ↘Flaky appearance	↗Thickness ↗Flaky appearance	↗Thickness ↗Flaky appearance Detachment by area

Non Significant: NS Significant: # $p < 0.1$; ** $p < 0.01$.

In the salicylic acid–treated sections, more pronounced histological alterations were observed, including increased cytoplasmic vacuolization and the presence of clear spaces between the epidermis and dermis, which are indicative of tissue and cellular alterations and are consistent with reduced tissue viability.

Interestingly, bSU treatment resulted in a reduction in SC thickness, whereas SA at the same concentrations induced a concentration-dependent increase in SC thickness. This divergence may be attributable to the stronger irritancy of SA. The acute barrier perturbation can trigger a compensatory repair response, leading to epidermal hyperproliferation or reactive hyperkeratosis [4,34]. Integrating the RHE findings, both compounds modulate the morphology of the SC; however, bSU facilitates exfoliation through a gentle loosening of intercorneocyte cohesion rather than through cellular damage or protein denaturation, thereby producing an exfoliating effect without compromising tissue integrity.

3.2.2. Homeostatic Regulation of SC Structure and Protein Expression

Analysis of the ex vivo skin tissues revealed distinct mechanistic features of bSU and SA in regulating desquamation-related proteins. A reduction of CDSN expression was observed, with both 1% and 3% bSU treatments, in agreement with the RHE model findings (Figure 9a), whereas SA at equivalent concentrations exerted minimal or no effect. Regarding DSG1, bSU treatment markedly increased its expression (Figure 9b), suggesting enhanced cohesion within the viable epidermal layers, whereas SA treatment led to a decrease in DSG1 expression. In addition, bSU induced a concentration-dependent reduction in LEKTI expression—mild at 1% and pronounced at 3%—while SA caused no evident change or only a slight increase (Figure 9c,d).

Consistent with the RHE findings, the exfoliating effect of bSU appears to align with the LEKTI–CDSN regulatory pathway, in which the reduction of CDSN promotes the physiological degradation of corneodesmosomes, enabling mild desquamation [43,44]. Notably, unlike SA, which tends to decrease DSG1 expression in the explant model, bSU markedly upregulated DSG1. A relatively reasonable explanation is that perturbation of the superficial epidermal structure triggers a form of stress-induced homeostatic regulation, leading to a structural compensatory response. Previous studies have shown that when the skin experiences barrier perturbation or mild insults, such as tape stripping [45], low-dose chemical exposure [46], or light stimulation—immune cells and keratinocytes coordinate multiple pathways to restore structural and functional homeostasis [47]. In this study, the bSU-induced increase in DSG1 may therefore represent an active, reparative adhesion-enhancing mechanism initiated in response to the superficial structural loosening caused by CDSN reduction. Such compensatory regulation may help partially maintain intercellular cohesion and structural integrity, thereby preventing further propagation of corneocyte detachment. However, given the multifactorial nature of epidermal regulation—including inflammatory mediators, metabolic status, redox balance, and the dynamics of keratinocyte differentiation [48]—and thus DSG1 upregulation is unlikely to arise solely from a structural compensation mechanism; further studies are needed to elucidate the underlying mechanisms fully.

In addition, the opposite LEKTI responses observed between RHE and ex vivo models likely reflect the physiological limitations of the RHE system. While the natural epidermal pH gradient spatially regulates desquamation through controlled LEKTI-KLK dissociation [10,49,50], the RHE model lacks key physiological components—including dermal vasculature, immune cell populations, lipid metabolic processes, and calcium gradient regulation [51,52]. Consequently, acid treatments likely act predominantly on the SC, without eliciting inward pH propagation or signaling coupling. Accordingly, the observed upregulation of LEKTI is more consistent with a stress-induced protective response to exogenous

stimuli [53], rather than a physiological regulation of desquamation homeostasis. In contrast, the native architecture of ex vivo skin supports more physiologically relevant protease regulation, where the natural pH gradient spatially controls LEKTI-KLK dissociation.

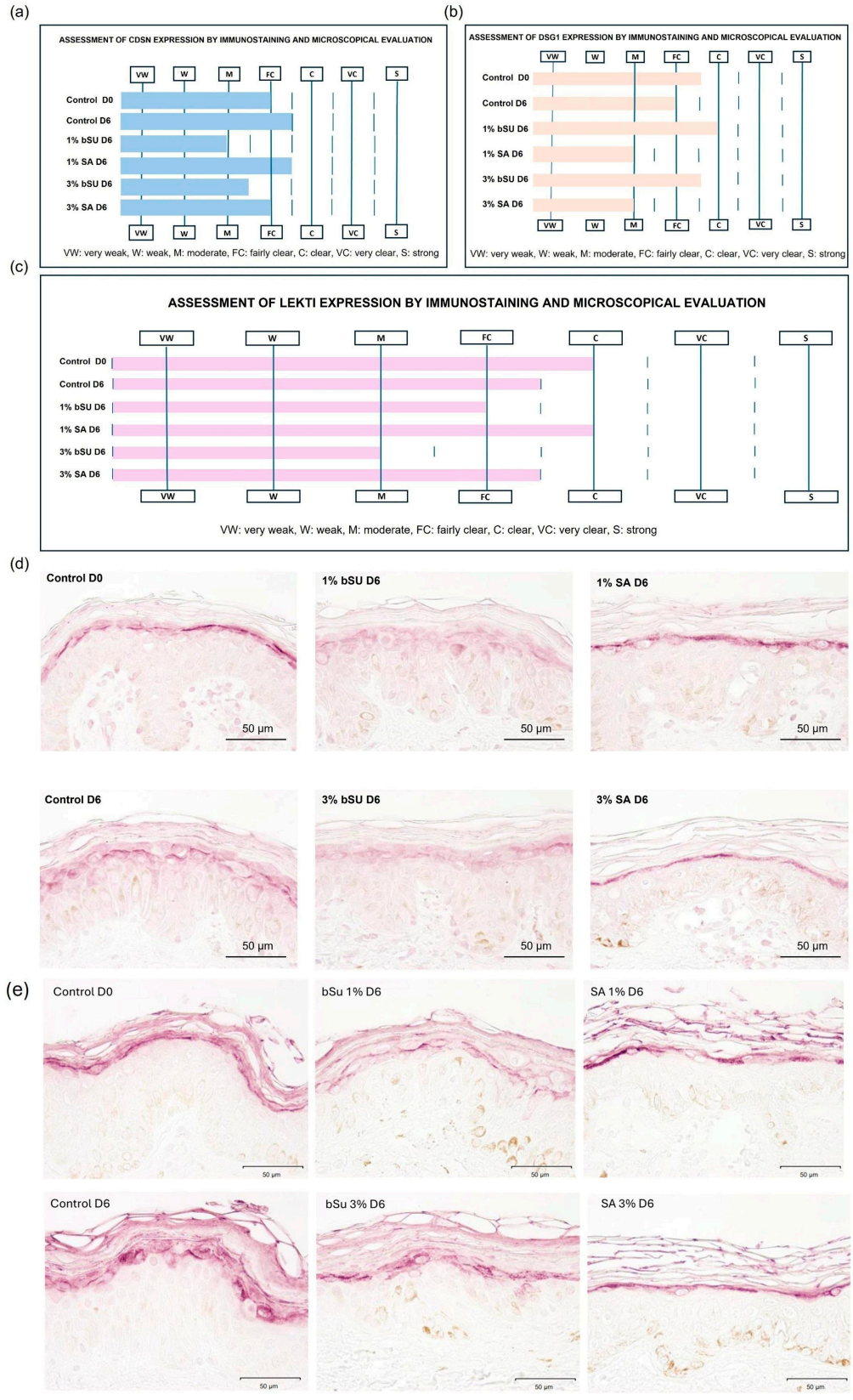

Figure 9. *Cont.*

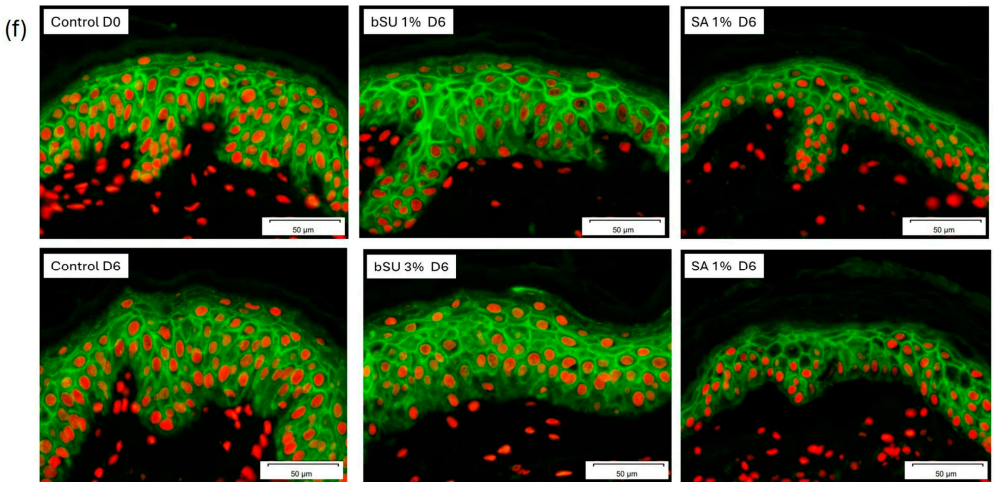

Figure 9. Assessment of (**a**) CDSN, (**b**) DSG1 and (**c**) LEKTI expression by immunostaining and microscopical evaluation after 6 days of treatment with 1% or 3% acids in human skin explants; Microscopical observation of the immunostaining staining of LEKTI (**d**), CDSN (**e**) (LEKTI and CDSN staining are shown in dark pink) and DSG1 (**f**) (DSG-1 staining is shown in green, and nuclei are shown in red) expressions and after 6 days treatment with 1% or 3% acids in human skin explants. $n = 3$.

3.2.3. Verification of Skin Barrier Function Homeostasis

The effects of bSU on skin barrier integrity were assessed by monitoring skin surface pH and TEWL ($g/m^2/h$). The results demonstrated a clear distinction between bSU and SA in their modulation of surface acidity. Specifically, bSU maintained the skin surface at a stable, physiologically relevant weakly acidic pH, whereas SA induced a pronounced pH drop of up to 3.5 units within 6 h, followed by marked instability and rebound (Figure 10). The buffering capacity of bSU is attributed to its two pKa values (4.2 and 5.6), which provide an effective buffering range spanning pH 4.4–5.8, enabling stable and sustained acidity control under mildly acidic conditions [54–56]. However, the buffering capacity was inferred based on pKa values and surface pH dynamics and was not directly quantified in this study.

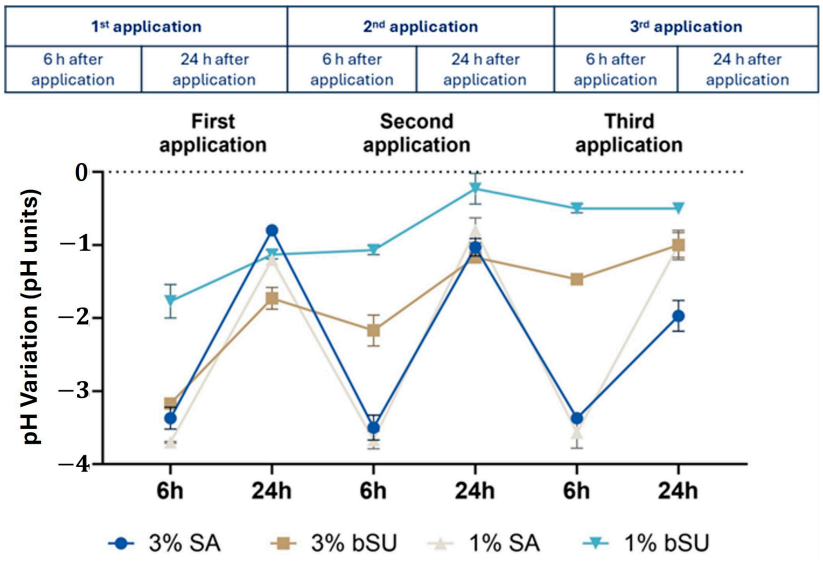

Figure 10. Effects of SA and bSU (1% and 3%) on skin pH of human skin explants at 6/24 h before and after application vs D0. $n = 3$. The skin pH was measured on the surface of the explants: On Day 0 (D0) before the application of any product; On D0, D3, and D5, 6 h after each treatment (after wiping the explants); On D1, D4, and D6, 24 h after each treatment.

TEWL measurements showed that treatment with bSU caused a slight and non-significant increase on D1, followed by a marked decrease from D4 to D6. In contrast, SA induced a continuous increase in TEWL up to D5 (Figure S1). It should be noted that TEWL reflects longitudinal changes in baseline barrier integrity rather than acute post-application responses.

Taken together, these findings suggest that bSU achieves a mild exfoliating effect through modulating corneodesmosomal structure, while avoiding the excessive degradation that typically results in barrier impairment. bSU's minimal impact on key barrier effector molecules, such as FLG, further supports its favorable tolerability in maintaining epidermal barrier function.

4. Conclusions

This study compared the effects of bSU and SA through in vitro and ex vivo human skin models. bSU demonstrated exfoliation efficacy comparable to SA but with markedly superior skin tolerance. Unlike SA—which induced stronger inflammation, reactive SC thickening, and surface pH instability—bSU preserved epidermal structure, maintained differentiation homeostasis, and generated only minimal inflammatory activation. bSU reduced CDSN expression, consistent with physiological promotion of corneodesmosomal degradation, while uniquely increasing DSG1 in human explants, indicating a compensatory adhesion-enhancing response that may contribute to improved barrier stability. Additionally, bSU maintained a physiologically relevant acidic pH, supporting its favorable impact on barrier homeostasis. A limitation of this study is that the test system was conducted in an aqueous solution rather than within a complete formulation matrix. However, the selected concentrations correspond to commonly used levels in commercial exfoliating products, providing practical relevance. Moreover, validation using RHE and human skin explant models enhances the physiological relevance and translational value of the findings. Overall, bSU represents a mild yet effective exfoliating active capable of modulating desquamation pathways without inducing cytotoxicity, irritation, or barrier impairment. Finally, clinical studies corroborated these in vitro findings through clinical trials involving 60 volunteers. Over a 28-day leave-on application period, the efficacy and tolerability of 2% bSU were compared with 2% SA and a placebo. Clinical assessments focused on comedone reduction and improvement in skin tone.

Results demonstrated that bSU enhanced skin radiance and reduced comedones. Notably, while using SA, 35% of participants reported irritation, sensations of tightness, and discomfort.

These advantages highlight bSU's potential as a safer alternative to traditional hydroxy acids.

Supplementary Materials: The following supporting information can be downloaded at: https://www.mdpi.com/article/10.3390/cosmetics13030119/s1, Figure S1: TEWL variation in human skin explants treated with 0.8% bSU or 0.8% SA. (a) TEWL changes from D1 to D6 relative to baseline (D0) for bSU and SA; (b) Comparison of TEWL variation (DX–D0) for bSU and SA vs. Controls.

Author Contributions: Conceptualization, G.L.-P., X.C. and Y.F.; methodology, Y.F.; validation, Y.F.; formal analysis, Q.Z.; investigation, Q.Z. and Y.F.; resources, G.L.-P. and X.C.; data curation, Q.Z. and Y.F.; writing—original draft preparation, M.G.; writing—review and editing, D.T., D.W., G.L.-P. and X.C.; visualization, M.G.; supervision, X.C.; project administration, G.L.-P. and X.C.; funding acquisition, G.L.-P. and X.C. All authors have read and agreed to the published version of the manuscript.

Funding: This research was supported by Proya and Roquette.

Institutional Review Board Statement: Not applicable.

Informed Consent Statement: Not applicable.

Data Availability Statement: The original contributions presented in this study are included in the article. Further inquiries can be directed to the corresponding author.

Acknowledgments: Roquette R&D Health & Nutrition, Cosmetic Technical Services, and Marketing and Communications departments, for their support, with special thanks to Leon MENTINK and Sophie CASTELAIN for their assistance and advice. Sophie CATOIRE and Adeline JOSSEAUME from Cell Alternativ, for their analysis and collaboration, and Laurent PENO-MAZZARIN from BIO-EC laboratories, for his analysis, collaboration, and advice.

Conflicts of Interest: Géraldine Louvet-Pommier, Daniel Wils and Damien Truffin the authors are employees of Roquette Frères. Yuanyuan Fang, Qian Zhang, Mengxue Gao, and Xiaowei Chang the authors are employees of Proya Cosmetics Co., Ltd. The authors declare that the research was conducted in the absence of any commercial or financial relationships that could be construed as a potential conflict of interest. The funders had no role in the design of the study; in the collection, analyses or interpretation of data; in the writing of the manuscript; or in the decision to publish the results.

References

1. Bouwstra, J.A.; Nadaban, A.; Bras, W.; McCabe, C.; Bunge, A.; Gooris, G.S. The skin barrier: An extraordinary interface with an exceptional lipid organization. *Prog. Lipid Res.* **2023**, *92*, 101252. [CrossRef]
2. Matsui, T.; Amagai, M. Dissecting the formation, structure and barrier function of the stratum corneum. *Int. Immunol.* **2015**, *27*, 269–280. [CrossRef] [PubMed]
3. Matsui, T.; Kadono-Maekubo, N.; Suzuki, Y.; Furuichi, Y.; Shiraga, K.; Sasaki, H.; Ishida, A.; Takahashi, S.; Okada, T.; Toyooka, K.; et al. A unique mode of keratinocyte death requires intracellular acidification. *Proc. Natl. Acad. Sci. USA* **2021**, *118*, e2020722118. [CrossRef] [PubMed]
4. Menon, G.K.; Cleary, G.W.; Lane, M.E. The structure and function of the stratum corneum. *Int. J. Pharm.* **2012**, *435*, 3–9. [CrossRef]
5. Stamatas, G.N. Protein degradation in the stratum corneum. *Int. J. Cosmet. Sci.* **2024**, *46*, 590–597. [CrossRef] [PubMed]
6. Morizane, S. The Role of Kallikrein-Related Peptidases in Atopic Dermatitis. *Acta Med. Okayama* **2019**, *73*, 1–6. [CrossRef]
7. Prassas, I.; Eissa, A.; Poda, G.; Diamandis, E.P. Unleashing the therapeutic potential of human kallikrein-related serine proteases. *Nat. Rev. Drug Discov.* **2015**, *14*, 183–202. [CrossRef]
8. Tanaka, R.J.; Ono, M.; Harrington, H.A. Skin barrier homeostasis in atopic dermatitis: Feedback regulation of kallikrein activity. *PLoS ONE* **2011**, *6*, e19895. [CrossRef]
9. Chen, J.Q.; Liang, B.H.; Li, H.P.; Mo, Z.Y.; Zhu, H.L. Roles of kallikrein-related peptidase in epidermal barrier function and related skin diseases. *Int. J. Dermatol. Venereol.* **2019**, *2*, 150–155. [CrossRef]
10. Matus, C.E.; Ehrenfeld, P.; Figueroa, C.D. The family of kallikrein-related peptidases and kinin peptides as modulators of epidermal homeostasis. *Am. J. Physiol. Cell Physiol.* **2022**, *323*, C1070–C1087. [CrossRef]
11. Jonca, N.; Guerrin, M.; Hadjiolova, K.; Caubet, C.; Gallinaro, H.; Simon, M.; Serre, G. Corneodesmosin, a component of epidermal corneocyte desmosomes, displays homophilic adhesive properties. *J. Biol. Chem.* **2002**, *277*, 5024–5029. [CrossRef]
12. Simon, M.; Jonca, N.; Guerrin, M.; Haftek, M.; Bernard, D.; Caubet, C.; Egelrud, T.; Schmidt, R.; Serre, G. Refined characterization of corneodesmosin proteolysis during terminal differentiation of human epidermis and its relationship to desquamation. *J. Biol. Chem.* **2001**, *276*, 20292–20299. [CrossRef]
13. Sotiropoulou, G.; Zingkou, E.; Pampalakis, G. Reconstructing the epidermal proteolytic cascades in health and disease. *J. Pathol.* **2022**, *257*, 545–560. [CrossRef]
14. Getsios, S.; Simpson, C.L.; Kojima, S.; Harmon, R.; Sheu, L.J.; Dusek, R.L.; Cornwell, M.; Green, K.J. Desmoglein 1-dependent suppression of EGFR signaling promotes epidermal differentiation and morphogenesis. *J. Cell Biol.* **2009**, *185*, 1243–1258. [CrossRef]
15. Naoe, Y.; Hata, T.; Tanigawa, K.; Kimura, H.; Masunaga, T. Bidimensional analysis of desmoglein 1 distribution on the outermost corneocytes provides the structural and functional information of the stratum corneum. *J. Dermatol. Sci.* **2010**, *57*, 192–198. [CrossRef]
16. Descargues, P.; Deraison, C.; Bonnart, C.; Kreft, M.; Kishibe, M.; Ishida-Yamamoto, A.; Elias, P.; Barrandon, Y.; Zambruno, G.; Sonnenberg, A.; et al. Spink5-deficient mice mimic Netherton syndrome through degradation of desmoglein 1 by epidermal protease hyperactivity. *Nat. Genet.* **2005**, *37*, 56–65. [CrossRef] [PubMed]
17. Vidal, S.I.; Menta, N.; Friedman, A. All Things Acids: A Primer on Alpha Hydroxy, Beta Hydroxy, and Polyhydroxy Acids. *J. Drugs Dermatol.* **2025**, *24*, 549–550.

18. Conneely, M.J.; Namkoong, J.; Allison, F.; Hirata Tsutsumi, S.K.; Grussu, D.; Willis, R.; Henderson, K.; Campbell, P.A.; Moy, M.; Lesniak, E.; et al. A Tensioned Human Skin Explant Model Used for Preliminary Assessment of Chemexfoliant-Stimulated Bioeffects. *JID Innov.* **2024**, *5*, 100305. [CrossRef] [PubMed]
19. Zhang, L.; Shao, X.; Chen, Y.; Wang, J.; Ariyawati, A.; Zhang, Y.; Chen, J.; Liu, L.; Pu, Y.; Li, Y.; et al. 30% supramolecular salicylic acid peels effectively treats acne vulgaris and reduces facial sebum. *J. Cosmet. Dermatol.* **2022**, *21*, 3398–3405. [CrossRef] [PubMed]
20. Green, B.A.; Yu, R.J.; Van Scott, E.J. Clinical and cosmeceutical uses of hydroxyacids. *Clin. Dermatol.* **2009**, *27*, 495–501. [CrossRef]
21. Kornhauser, A.; Coelho, S.G.; Hearing, V.J. Applications of hydroxy acids: Classification, mechanisms, and photoactivity. *Clin. Cosmet. Investig. Dermatol.* **2010**, *3*, 135–142. [CrossRef] [PubMed]
22. Arif, T. Salicylic acid as a peeling agent: A comprehensive review. *Clin. Cosmet. Investig. Dermatol.* **2015**, *8*, 455–461. [CrossRef]
23. Johnson, W., Jr.; Zhu, J.; Bergfeld, W.F.; Belsito, D.V.; Hill, R.A.; Klaassen, C.D.; Liebler, D.C.; Marks, J.G., Jr.; Shank, R.C.; Slaga, T.J.; et al. Amended Safety Assessment of Salicylic Acid and Salicylates as Used in Cosmetics. *Int. J. Toxicol.* **2025**, *44*, 5S–57S. [CrossRef]
24. Tang, S.C.; Yang, J.H. Dual Effects of Alpha-Hydroxy Acids on the Skin. *Molecules* **2018**, *23*, 863. [CrossRef]
25. Nissen, M.D.; Lau, E.T.L.; Cabot, P.J.; Steadman, K.J. Baltic amber teething necklaces: Could succinic acid leaching from beads provide anti-inflammatory effects? *BMC Complement. Altern. Med.* **2019**, *19*, 162. [CrossRef]
26. Chien, S.C.; Chen, M.L.; Kuo, H.T.; Tsai, Y.C.; Lin, B.F.; Kuo, Y.H. Anti-inflammatory activities of new succinic and maleic derivatives from the fruiting body of Antrodia camphorata. *J. Agric. Food Chem.* **2008**, *56*, 7017–7022. [CrossRef]
27. Fumagalli, C. Updated by Staff. Succinic Acid and Succinic Anhydride. In *Kirk-Othmer Encyclopedia of Chemical Technology*; John Wiley & Sons, Inc.: Hoboken, NJ, USA, 2000.
28. Nghiem, N.P.; Kleff, S.; Schwegmann, S. Succinic Acid: Technology Development and Commercialization. *Fermentation* **2017**, *3*, 26. [CrossRef]
29. Martinez-Gutierrez, A.; Cami, H.; Noya, T.; Gomez-Escalante, S.; Miro Llosas, A.; Gonzalez, M.C. Hyaluronic and Succinic Acid: New Biostimulating Combination to Counteract Dermal and Subcutaneous Aging. *Int. J. Mol. Sci.* **2025**, *26*, 7548. [CrossRef] [PubMed]
30. Kumar, V.; Kumar, P.; Maity, S.K.; Agrawal, D.; Narisetty, V.; Jacob, S.; Kumar, G.; Bhatia, S.K.; Kumar, D.; Vivekanand, V. Recent advances in bio-based production of top platform chemical, succinic acid: An alternative to conventional chemistry. *Biotechnol. Biofuels Bioprod.* **2024**, *17*, 72. [CrossRef] [PubMed]
31. Neil, J.E.; Brown, M.B.; Williams, A.C. Human skin explant model for the investigation of topical therapeutics. *Sci. Rep.* **2020**, *10*, 21192. [CrossRef]
32. Niehues, H.; Bouwstra, J.A.; El Ghalbzouri, A.; Brandner, J.M.; Zeeuwen, P.; van den Bogaard, E.H. 3D skin models for 3R research: The potential of 3D reconstructed skin models to study skin barrier function. *Exp. Dermatol.* **2018**, *27*, 501–511. [CrossRef] [PubMed]
33. Patrick, M.; Gallic, B.; Laurent, P.M.; Elian, L.; Richard, F.; Katell, V. Assessment of an ex vivo irritation test performed on human skin explants and comparison of its results with those of a 24-/48-h human patch test for the evaluation of cosmetics. *Toxicol. In Vitro* **2021**, *70*, 105030. [CrossRef]
34. Yang, L.; Wang, S.; Pan, H.; Zhou, X.; Wei, J.; Zhou, M.; Yang, Y.; Quan, Q. Glycolic acid-induced disruption of epidermal homeostasis in a skin equivalent model: Insights into temporal dynamics and mechanisms. *Toxicol. Lett.* **2024**, *397*, 1–10. [CrossRef]
35. Chou, C.C.; Huang, T.L.; Pan, C.Y. Atomistic simulation of mutation effect on the hierarchical structure and mechanics of human epithelial keratin K1/K10. *Biophys. J.* **2022**, *121*, 322a. [CrossRef]
36. Tsubota, A.; Akiyama, M.; Sakai, K.; Goto, M.; Nomura, Y.; Ando, S.; Abe, M.; Sawamura, D.; Shimizu, H. Keratin 1 gene mutation detected in epidermal nevus with epidermolytic hyperkeratosis. *J. Investig. Dermatol.* **2007**, *127*, 1371–1374. [CrossRef]
37. Ekholm, I.E.; Brattsand, M.; Egelrud, T. Stratum corneum tryptic enzyme in normal epidermis: A missing link in the desquamation process? *J. Investig. Dermatol.* **2000**, *114*, 56–63. [CrossRef] [PubMed]
38. Rawlings, A.V.; Matts, P.J. Stratum corneum moisturization at the molecular level: An update in relation to the dry skin cycle. *J. Investig. Dermatol.* **2005**, *124*, 1099–1110. [CrossRef]
39. Sandilands, A.; Sutherland, C.; Irvine, A.D.; McLean, W.H. Filaggrin in the frontline: Role in skin barrier function and disease. *J. Cell Sci.* **2009**, *122*, 1285–1294. [CrossRef]
40. Stefanovic, N.; Irvine, A.D. Filaggrin and beyond: New insights into the skin barrier in atopic dermatitis and allergic diseases, from genetics to therapeutic perspectives. *Ann. Allergy Asthma Immunol.* **2024**, *132*, 187–195. [CrossRef]
41. Ozdemir, E.; Oksuz, L. Effect of *Staphylococcus aureus* colonization and immune defects on the pathogenesis of atopic dermatitis. *Arch. Microbiol.* **2024**, *206*, 410. [CrossRef]
42. Schafer-Korting, M.; Mahmoud, A.; Lombardi Borgia, S.; Bruggener, B.; Kleuser, B.; Schreiber, S.; Mehnert, W. Reconstructed epidermis and full-thickness skin for absorption testing: Influence of the vehicles used on steroid permeation. *Altern. Lab. Anim.* **2008**, *36*, 441–452. [CrossRef]

43. van der Velden, J.; van Geel, M.; Engelhart, J.J.; Jonkman, M.F.; Steijlen, P.M. Mutations in the CDSN gene cause peeling skin disease and hypotrichosis simplex of the scalp. *J. Dermatol.* **2020**, *47*, 3–7. [CrossRef] [PubMed]
44. Tsukui, K.; Suzuki, M.; Amma, M.; Kawaguchi, S.I.; Tokudome, Y. Dual Regulation of Corneodesmosome Formation by Shotokuseki Extract Enhances Skin Barrier Homeostasis. *Molecules* **2025**, *30*, 4592. [CrossRef]
45. Man, M.-Q.; Gao, J.-F.; Zhang, G.-Q. Co-Regulation of Epidermal Permeability Barrier Function and Immune Function: A Narrative Review. *Int. J. Dermatol. Venereol.* **2025**, *08*, 166–174. [CrossRef]
46. Drigeard Desgarnier, M.C.; Fournier, F.; Droit, A.; Rochette, P.J. Influence of a pre-stimulation with chronic low-dose UVB on stress response mechanisms in human skin fibroblasts. *PLoS ONE* **2017**, *12*, e0173740. [CrossRef]
47. Jiao, Q.; Zhi, L.; You, B.; Wang, G.; Wu, N.; Jia, Y. Skin homeostasis: Mechanism and influencing factors. *J. Cosmet. Dermatol.* **2024**, *23*, 1518–1526. [CrossRef] [PubMed]
48. Cetinarslan, T.; Kumper, L.; Folster-Holst, R. The immunological and structural epidermal barrier dysfunction and skin microbiome in atopic dermatitis-an update. *Front. Mol. Biosci.* **2023**, *10*, 1159404. [CrossRef]
49. Thibault Greugny, E.; Bensaci, J.; Fages, F.; Stamatas, G.N. Computational modelling predicts impaired barrier function and higher sensitivity to skin inflammation following pH elevation. *Exp. Dermatol.* **2023**, *32*, 177–185. [CrossRef]
50. Elias, P.M. The epidermal permeability barrier: From the early days at Harvard to emerging concepts. *J. Investig. Dermatol.* **2004**, *122*, xxxvi–xxxix. [CrossRef]
51. Yip, S.; Wang, N.; Sugimura, R. Give Them Vasculature and Immune Cells: How to Fill the Gap of Organoids. *Cells Tissues Organs* **2023**, *212*, 369–382. [CrossRef]
52. Hagvall, L.; Munem, M.; Hoang Philipsen, M.; Dowlatshahi Pour, M.; Hedberg, Y.; Malmberg, P. Skin permeation studies of chromium species—Evaluation of a reconstructed human epidermis model. *Toxicol. In Vitro* **2023**, *91*, 105636. [CrossRef] [PubMed]
53. Jiang, Y.; Tsoi, L.C.; Billi, A.C.; Ward, N.L.; Harms, P.W.; Zeng, C.; Maverakis, E.; Kahlenberg, J.M.; Gudjonsson, J.E. Cytokinocytes: The diverse contribution of keratinocytes to immune responses in skin. *JCI Insight* **2020**, *5*, e142067. [CrossRef]
54. Sundaramurthi, P.; Suryanarayanan, R. Thermophysical properties of carboxylic and amino acid buffers at subzero temperatures: Relevance to frozen state stabilization. *J. Phys. Chem. B* **2011**, *115*, 7154–7164. [CrossRef] [PubMed]
55. Almbrok, E.M.; Abdelkader, H.; Mohamed, A. Mixed Metal Complexes of Succinic Acid: The Effect of PH and Ionic Speciation Modeling. *Aajsr* **2025**, *3*, 109–114.
56. Ukidve, A.; Rembert, K.B.; Vanipenta, R.; Dorion, P.; Lafarguette, P.; McCoy, T.; Saluja, A.; Suryanarayanan, R.; Patke, S. Succinate Buffer in Biologics Products: Real-world Formulation Considerations, Processing Risks and Mitigation Strategies. *J. Pharm. Sci.* **2023**, *112*, 138–147. [CrossRef]

Disclaimer/Publisher's Note: The statements, opinions and data contained in all publications are solely those of the individual author(s) and contributor(s) and not of MDPI and/or the editor(s). MDPI and/or the editor(s) disclaim responsibility for any injury to people or property resulting from any ideas, methods, instructions or products referred to in the content.